On the Impact of Misalignment Fading in Transdermal Optical Wireless Communications

Stylianos E. Trevlakis[1], Alexandros – Apostolos A. Boulogeorgos[1,2], and George K. Karagiannidis[1]
[1]Department of Electrical and Computer Engineering, Aristotle University of Thessaloniki, 54124 Thessaloniki, Greece
[2]Department of Digital Systems, University of Piraeus, Piraeus 18534, Greece
e-mails: {trevlakis; geokarag}@auth.gr; al.boulogeorgos@ieee.org

***Abstract*—In this paper, we study the performance of the transdermal optical wireless communications (OWCs). In order to provide a quantified understanding of the link's parameters, we establish an appropriate theoretical framework that takes into account the channel particularities, the integration area of the internal unit, the transmitter-receiver misalignment, and the characteristics of the optical units. In more detail, we present closed-form expressions for the instantaneous and average signal to noise ratio (SNR) of the OWCs transdermal link. The findings reveal that misalignment fading drastically affects the reliability and effectiveness of the transdermal link.**

I. Introduction

Recently, medical implants have been a subject of much hype, due to the quality of life improvements that they offer. Convetional medical implants employ near-field magnetic communication technologies, operate at low RF frequencies, with transmission power in the order of some decades mWatt [1]. However these implants cannot support high data rates, which are necessary for achieving performance similar to the human organs with reasonable transmission power [2], [3]. Furthermore, in combination with the interference from other sources operating in the medical implants communication service frequency band, the RF transmission is considered to be a mediocre solution [4], [5].

In order to break these barriers, one needs to investigate the feasibility of transdermal wireless links operating in non-standardized frequency bands. In this sense, and due to the large bandwidths available, the partial transparency of skin at infrared wavelengths and the extremely high immunity to external interference, the use of optical wireless communications (OWCs) was recently introduced as an attractive alternative (see [6]–[9] and references therein). The feasibility of OWCs for the transcutaneous link was experimentally validated in several papers [10]–[13]. In more detail, in [10], optical wireless links were used to establish transdermal high data rate communications between the internal and external unit of the medical system, whereas, in [11], experimental results of direct and retroreflection transdermal link configurations were presented. Additionally, in [12], the authors evaluated the system model of a transdermal optical link with regard to tissue thickness, data rate and transmitted power.

However, in most of the previously mentioned papers, the impact of misalignment fading was neglected. On the other hand, in [4], [13], the authors investigated its effect in terms of bit error rate (BER). Specifically, in [4], a low power, high data rate optical wireless link was evaluated in terms of power consumption and BER, for a given misalignment tolerance. Finally, in [13], the authors verified in-vivo the feasibility of the transcutaneous optical link, proving that high data rate can be delivered with BER of 2×10^{-7} in the presence of misalignment.

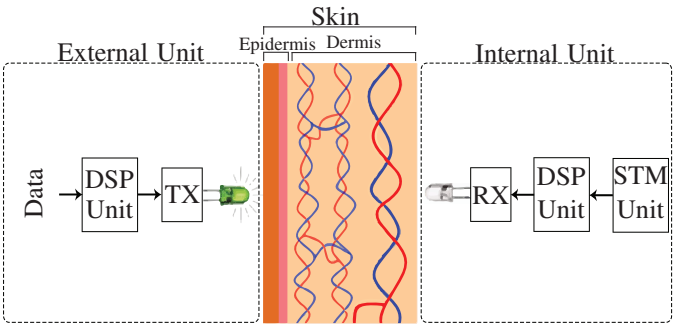

Fig. 1: System model.

However, in all of the above published papers, deterministic models were employed to accomodate the impact of misalignment. As a result, these models do not take into account the stochastic nature of misalignment, due to the relative motion between the transmitter (TX) and the receiver (RX). Motivated by this, in this paper, we quantify the impact of misalignment fading in terms of average SNR. In more detail, we present closed form expressions for the instantaneous and average SNR that take into account the transdermal channel particularities, the transceivers characteristics as well as the intensity of misalignment fading. The derived expressions provide important technical insights and can be used for OWC transdermal systems' design purposes.

II. System Model

As illustrated in Fig. 1, the main components of a medical implant system are the external unit, the propagation medium (skin) and the internal unit. We assume that the external unit consists of a data capturing unit, followed by the the digital signal processing (DSP) unit. The data capturing unit converts external stimulations into electrical signals, while the DSP unit is responsible for the digitization and compression of the data into modulated signals. These signals are forwarded to the TX, which sends the data to the RX, at the internal unit. The internal unit consists of the RX,a DSP unit, and a

978-1-5386-4788-2/18/$31.00 ©2018 IEEE

stimulation (STM) unit. The internal DSP and STM units are working together in order to translate the received signal into appropriate stimulations.

We assume that the transmitted signal, x, convey over a wireless channel, h, with additive noise n. Hence, the baseband equivalent received signal can be expressed as

$$y = Rhx + n, \tag{1}$$

where R stands for the responsivity of the RX's photodiode and can be obtained as $R = \eta\frac{q}{pv}$, with, η being the quantum efficiency of the photodiode, v the photons' frequency and p the Planck constant.

The channel, h, can be expressed as in [11], i.e., $h = h_l h_p$, where h_l and h_p respectively stand for the deterministic channel coefficient, due to the propagation loss, and the stochastic process that models the geometric spread, because of the so called "misalignment fading". The deterministic term of the channel coefficient can be expressed as [7, eq. 10.1]

$$h_l = \exp\left(-\frac{1}{2}\alpha(\lambda)\delta\right), \tag{2}$$

where $\alpha(\lambda)$ and δ represent the skin attenuation coefficient in the wavelength λ[1], and the total dermis thickness, respectively.

The noise component can be expressed as $n = n_b + n_{DC} + n_t$, where n_b, and n_{DC} stand for the background shot noise, dark current shot noise, respectively, which can be modeled as zero-mean Gaussian processes with variances $\sigma_b^2 = 2qRBP_b$ and $\sigma_{DC}^2 = 2qBI_{DC}$, where q is the electron charge, B is the communication bandwidth, P_b is the background optical power, and I_{DC} is the intensity of the dark current. Finally, n_t represents the thermal noise, which is also modelled as a zero-mean Gaussian process with variance σ_t^2. Note that, since n_b, n_{DC}, and n_t are zero-mean Gaussian processes [11], n also follows zero-mean Gaussian distribution with variance

$$\sigma^2 = \sigma_b^2 + \sigma_{DC}^2 + \sigma_t^2. \tag{3}$$

III. Average SNR

Based on (1)-(3), and by assuming an intensity modulation and direct detection (IM/DD) method, the instantaneous SNR can be obtained as [16]

$$\gamma = \frac{R^2 \exp\left(-\alpha(\lambda)\delta\right) h_p^2 P_s}{2qRBP_b + 2qBI_{DC} + \sigma_t^2}, \tag{4}$$

$$= \frac{R^2 \exp\left(-\alpha(\lambda)\delta\right) h_p^2 \tilde{P}_s}{2qRP_b + 2qI_{DC} + N_0}, \tag{5}$$

where P_s denotes the average optical power of the transmitted signal, whereas $\tilde{P}_s$ and N_0 respectively represent the signal and noise optical power spectral density (PSD).

Theorem 1: The average SNR, can be obtained as

$$\tilde{\gamma} = \frac{R^2 \exp\left(-\alpha(\lambda)\delta\right) \tilde{P}_s}{2qRP_b + 2qI_{DC} + N_0} \frac{\xi A_0^2}{\xi + 2}, \tag{6}$$

[1]The values of $\alpha(\lambda)$ depends on the optical properties of the skin and can be obtained from [14], [15].

where A_0 stand for the the fraction of the collected power in case of zero radial displacement and can be expressed as in [17]

$$A_0 = \mathrm{erf}\left(\upsilon\right)^2, \tag{7}$$

with

$$\upsilon = \frac{\sqrt{\pi}\beta}{\sqrt{2}w_\delta}. \tag{8}$$

In (8), β and w_δ respectively denote the radius of the RX's circular aperture and the beam waste (radius calculated at e^{-2}) on the RX plane at distance δ from the TX. Moreover, in (6), ξ is the square ratio of the equivalent beam radius, w_{eq}, and the pointing error displacement standard deviation at the RX, and can be expressed as

$$\xi = \frac{w_{eq}^2}{4\sigma_s^2}, \tag{9}$$

where σ_s^2 is the pointing error displacement (jitter) variance at the RX. Finally, note that w_{eq}^2 can be evaluated as

$$w_{eq}^2 = w_\delta^2 \frac{\sqrt{\pi}\,\mathrm{erf}\left(\upsilon\right)}{2\upsilon \exp\left(-\upsilon^2\right)}. \tag{10}$$

Proof: Please refer to the Appendix. ■

From (6), it is evident that the average SNR depends on the transmission PSD, the skin particularities, namely skin attenuation and thickness, the RX's characteristics, and the intensity of the misalignment fading. Moreover, note that, since the skin attenuation is a function of the wavelength, the average SNR is also a function of the wavelength.

IV. Results and Discussion

In this section, we evaluate the performance of the transdermal OWC link by illustrating analytical and Monte-Carlo simulation results for different insightful scenarios. In more detail, we assume that the photodiode effective area, A, which is defined as $A = \pi\beta^2$, is $1\ \mathrm{mm}^2$, while the divergence angle, θ, equals 20^o. Additionally, unless otherwise is stated, the skin thickness, δ, is assumed to be equal to $4\ \mathrm{mm}$, while the noise optical PSD, N_0, is set to $\left(1.3\ \mathrm{pA}/\sqrt{\mathrm{Hz}}\right)^2$ [18]. The beam waist in distance δ is calculated as $w_\delta = \delta \tan\left(\frac{\theta}{2}\right)$. Moreover, according to [11], the OWC link shows extremely high immunity to external interference; hence, the background optical power can be omitted, i.e., $P_b = 0$. Furthermore, the photodiode's dark current, I_{DC}, is set to $0.05\ \mathrm{nA}$, whereas, $\eta = 0.8$ [7]. Finally, unless stated otherwise, we assume $\tilde{P}_s = 0.1\ \mu\mathrm{W/MHz}$, $\lambda = 1100\ \mathrm{nm}$ and $\xi = 1$.

Fig. 2 depicts the average SNR as a function of the wavelength for different values of the jitter standard deviation, σ_s. We observe that, although, the signal PSD in the OWCs is much lower compared to the one, when RF link is used, the average SNR is surprisingly high, i.e., in the order of $90\ dB$. This indicates that the OWCs can achieve much higher energy efficiency compared to the corresponding RF link. Moreover, for a fixed wavelength, as σ_s increases,

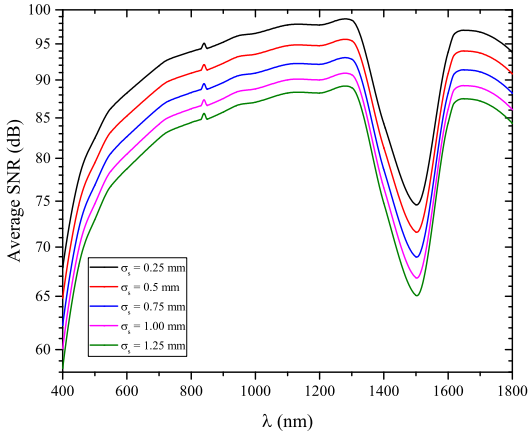

Fig. 2: Average SNR vs λ for different values of σ_s.

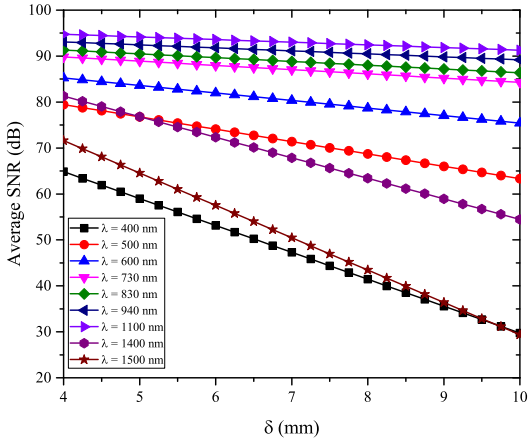

Fig. 3: Average SNR vs δ for different λ.

the average SNR decreases. For $\lambda = 600$ nm, the average SNR decreases approximately 10% as σ_s is altered from 0.25 to 1.25. Additionally, from this figure, it is evident that a transmission window exists for wavelengths between 700 and 1300 nm. Note that, in this wavelength region several commercial light emitting diodes (LEDs) and photodetectors (PD) exist (see for example [19], [20]). Finally, we observe that the wavelength windows from 400 to 600 nm and around 1500 nm are not optimal for OWCIs, whereas the optimal transmission wavelength is 1100 nm.

Fig. 3 demonstrates the impact of skin thickness on the received signal quality in the OWC link operating in different wavelengths. We observe that the analytical and simulation results coincide; therefore, the analytical framework for the derivation of the average SNR is verified. As expected, for a given wavelength, as the skin thickness increases, the average SNR decreases, i.e., the received signal quality degrades. This degradation is caused due to the pathloss. Additionally, we observe that, for a given skin thickness, δ, the average SNR depends on the wavelength. For example, for $\delta = 6$ mm and $\lambda = 1500$ nm, the average SNR equals 57.5 dB, whereas, for the same δ and $\lambda = 1400$ nm, the average SNR is 72.34 dB. In other words, the 100 nm variation of the wavelength, from 1500 to 1400 nm, resulted in a 25.8% signal quality improvement. On the other hand, for the same δ, when λ alters from 400 to 500 nm, the average SNR increases about 39.4%. This observation indicates the wavelength selectivity of the transdermal link, as well as the importance of appropriately choosing the wavelength, when designing the link. Finally, for $\delta \leq 5.25$ mm, we observe that a 1500 nm OWC link outperforms the corresponding link operating in 400 nm, while, for $\delta > 5.25$ mm, the opposite is valid. This is because, in these scenarios and for skin thickness lesser that 5.25 mm, the factor that determines the received signal quality degradation is mainly the RX's responsivity, whereas, for $\delta > 5.25$, the dominant factor is the skin attenuation coefficient.

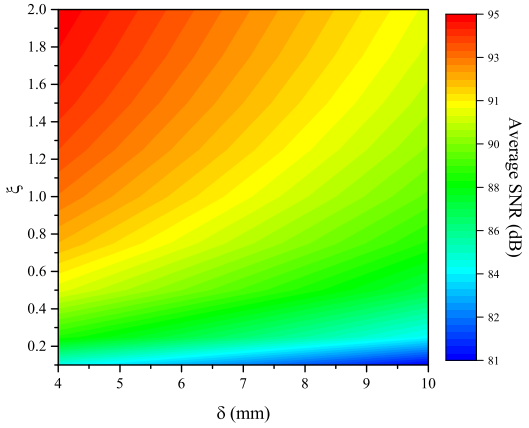

Fig. 4: Average SNR vs δ and ξ, with $\lambda = 940$ nm.

Fig. 4 illustrates the effect of skin thickness and misalignment fading in the received signal quality in terms of average SNR, for $\lambda = 940$ nm. From this figure, it is evident that, for a fixed ξ, as the skin thickness increases, the average SNR decreases. For instance, for $\xi = 0.5$, the SNR decreases from 90.18 to 87.57 dB, as the skin thickness increases from 5 mm to 9 mm, whereas, for $\xi = 2$, the SNR decreases from 94.16 to 91.55 dB, for the same skin thickness variation. This indicates that the average SNR degradation, due to skin thickness increase, is independent of the intensity of the misalignment fading. Additionally, from this figure, we see that, for a fixed skin thickness, as ξ increases, i.e., the intensity of misalignment fading decreases, the average SNR increases. For example, for $\delta = 0.7$ mm, when ξ alters from 0.1 to 1.5, the average SNR increases for about 10 dB, from 82.64 dB to 92.19 dB. Finally, we observe that for practical values of δ and ξ, i.e., $\delta \in [4, 10]$ mm and $\xi \in [0.1, 2]$, the achievable average SNR is very high, despite of the fact that the transmission PSD is respectively low.

V. Conclusions

In this paper, we presented novel closed-form expressions for the SNR in transdermal OWCs, which take into account the channel particularities, the characteristics of the optical transceivers and the TX-RX misalignment fading. Our findings

revealed that a transmission window exists for wavelengths between 700 and 1300 nm, while, the optimal transmission wavelength is 1100 nm. Finally, we quantified the detrimental effect of misalignment fading, which can degrade the transdermal OWC performance more than 10%.

APPENDIX

According to (5), the instantaneous SNR is a random variable (RV) that follows the same distribution as h_p^2. Therefore, in order to derive the average SNR of the optical link, we first need to identify the distribution of h_p^2.

By assuming that the spatial intensity of w_δ on the RX plane at distance δ from the TX and circular aperture of radius β, the stochastic term of the channel coefficient, which represents the fraction of the collected power due to geometric spread with radial displacement r from the origin of the detector, can be approximated as in [21],

$$h_p \approx A_0 \exp\left(-\frac{2r^2}{w_{eq}^2}\right). \tag{11}$$

Moreover, by assuming that the elevation and the horizontal displacement (sway) follow independent identical Gaussian distributions, as was done in previous work [22], we observe that the radial displacement at the RX follows a Rayleigh distribution, with a probability density function (PDF) given by

$$f_r(r) = \frac{r}{\sigma_s^2}\exp\left(-\frac{r^2}{2\sigma_s^2}\right), \qquad r > 0 \tag{12}$$

By combining the expressions (11) and (12), the PDF of h_p can be expressed as

$$f_{h_p}(x) = \frac{\xi}{A_0^\xi} x^{\xi-1}, \qquad 0 \le x \le A_0, \tag{13}$$

while, its cumulative distribution function (CDF) can be obtained as

$$F_{h_p}(x) \triangleq \int_0^x f_{h_p}(y)\,\mathrm{d}y = \begin{cases} \frac{1}{A_0^\xi}x^\xi & 0 \le x \le A_0 \\ 1, & x \ge A_0 \end{cases}. \tag{14}$$

The CDF of h_p^2 can be obtained as

$$\begin{aligned} F_{h_p^2}(x) &= P\left(h_p^2 \le x\right) = P\left(h_p \le \sqrt{x}\right) \\ &= P\left(h_p \le \sqrt{x}\right) = F_{h_p}\left(\sqrt{x}\right), \end{aligned} \tag{15}$$

which, by using (14), can be rewritten as

$$F_{h_p^2}(x) = \begin{cases} \frac{1}{A_0^\xi}x^{\xi/2} & 0 \le x \le A_0^2 \\ 1, & x \ge A_0^2 \end{cases}, \tag{16}$$

while, the PDF of h_p^2 can be obtained as

$$f_{h_p^2}(x) = \frac{\mathrm{d}F_{h_p^2}(x)}{\mathrm{d}x} = \frac{\xi}{2A_0^\xi}x^{\xi/2-1}. \tag{17}$$

The average SNR can be defined as $\tilde{\gamma} = \mathbb{E}[\gamma]$, which by using (5) and (17), can be written as

$$\tilde{\gamma} = \frac{R^2\exp\left(-\alpha(\lambda)\delta\right)\tilde{P}_s}{2qRP_b + 2qI_{DC} + N_0}\frac{\xi}{2A_0^\xi}\int_0^{A_0^2} x^{\xi/2}\mathrm{d}x, \tag{18}$$

By performing the integration, (18) can equivalently be written as (6). This concludes the proof.

REFERENCES

[1] K. Agarwal, R. Jegadeesan, Y. X. Guo, and N. V. Thakor, "Wireless power transfer strategies for implantable bioelectronics," *IEEE Rev. Biomed. Eng.*, vol. 10, pp. 136–161, Mar. 2017.

[2] H. J. Kim, H. Hirayama, S. Kim, K. J. Han, R. Zhang, and J. W. Choi, "Review of near-field wireless power and communication for biomedical applications," *IEEE Access*, vol. 5, pp. 21 264–21 285, Sep. 2017.

[3] A. C. Thompson, S. A. Wade, N. C. Pawsey, and P. R. Stoddart, "Infrared neural stimulation: Influence of stimulation site spacing and repetition rates on heating," *IEEE Trans. Biomed. Eng.*, vol. 60, no. 12, pp. 3534–3541, Dec. 2013.

[4] T. Liu, U. Bihr, S. M. Anis, and M. Ortmanns, "Optical transcutaneous link for low power, high data rate telemetry," in *Annual International Conference of the IEEE Engineering in Medicine and Biology Society (EMBC)*. IEEE, Aug. 2012, pp. 3535–3538.

[5] S. L. Pinski and R. G. Trohman, "Interference in implanted cardiac devices, part i," *Pacing Clin Electrophysiol*, vol. 25, no. 9, pp. 1367–1381, Sep. 2002.

[6] Z. Ghassemlooy, S. Arnon, M. Uysal, Z. Xu, and J. Cheng, "Emerging optical wireless communications-advances and challenges," *IEEE J. Sel. Areas Commun.*, vol. 33, no. 9, pp. 1738–1749, Sep. 2015.

[7] M. Faria, L. N. Alves, and P. S. de Brito André, *Transdermal Optical Communications*. CRC Press, Jun. 2017, vol. 1, ch. 10, pp. 309–336.

[8] G. K. Karagiannidis, T. A. Tsiftsis, and H. G. Sandalidis, "Outage probability of relayed free space optical communication systems," *Electronics Letters*, vol. 42, no. 17, pp. 994–996, Aug. 2006.

[9] N. D. Chatzidiamantis, G. K. Karagiannidis, and M. Uysal, "Generalized maximum-likelihood sequence detection for photon-counting free space optical systems," *IEEE Transactions on Communications*, vol. 58, no. 12, pp. 3381–3385, Dec. 2010.

[10] J. L. Abita and W. Schneider, "Transdermal optical communications," *JOHNS HOPKINS APL TECHNICAL DIGEST*, vol. 25, no. 3, p. 261, 2004.

[11] Y. Gil, N. Rotter, and S. Arnon, "Feasibility of retroreflective transdermal optical wireless communication," *Appl Opt*, vol. 51, no. 18, pp. 4232–4239, Jun. 2012.

[12] T. Liu, J. Anders, and M. Ortmanns, "System level model for transcutaneous optical telemetric link," in *IEEE International Symposium on Circuits and Systems (ISCAS)*, May 2013, pp. 865–868.

[13] T. Liu, U. Bihr, J. Becker, J. Anders, and M. Ortmanns, "In vivo verification of a 100 mbps transcutaneous optical telemetric link," in *IEEE Biomedical Circuits and Systems Conference (BioCAS)*, Oct. 2014, pp. 580–583.

[14] A. N. Bashkatov, E. A. Genina, and V. V. Tuchin, "Optical properties of skin, subcutaneous, and muscle tissues: a review," *Journal of Innovative Optical Health Sciences*, vol. 4, no. 01, pp. 9–38, Jan. 2011.

[15] A. Bashkatov, E. Genina, V. Kochubey, and V. Tuchin, "Optical properties of human skin, subcutaneous and mucous tissues in the wavelength range from 400 to 2000 nm," *J. Phys. D: Appl. Phys.*, vol. 38, no. 15, p. 2543, Jul. 2005.

[16] S. Arnon, J. Barry, G. Karagiannidis, R. Schober, and M. Uysal, Eds., *Advanced Optical Wireless Communication Systems*, 1st ed. New York, NY, USA: Cambridge University Press, May 2012.

[17] A. A. Farid and S. Hranilovic, "Outage capacity optimization for free-space optical links with pointing errors," *J. Lightwave Technol.*, vol. 25, no. 7, pp. 1702–1710, Jul. 2007.

[18] *155Mbps Low-Noise Transimpedance Amplifier*, Maxim Integrated Products, Feb. 2004, rev. 2.

[19] *High Speed Infrared Emitting Diode, 830 nm, GaAlAs Double Hetero*, Vishay Semiconductors, Aug. 2011, rev. 1.2.

[20] *Infrared (IR) Emitter 940nm 1.2V 100mA 7.8mW/sr @ 20mA 20° Radial*, Everlight Electronics Co Ltd, Dec. 2016, rev. 5.

[21] H. G. Sandalidis, T. A. Tsiftsis, G. K. Karagiannidis, and M. Uysal, "Ber performance of FSO links over strong atmospheric turbulence channels with pointing errors," *IEEE Commun. Lett.*, vol. 12, no. 1, pp. 44–46, Jan. 2008.

[22] S. Arnon, "Effects of atmospheric turbulence and building sway on optical wireless-communication systems," *Opt. Lett.*, vol. 28, no. 2, pp. 129–131, Jan. 2003.